Embedded cluster calculations of metal complex impurity defects: properties of the iron cyanide in NaCl

2000 J. Phys.: Condens. Matter 12 8257

(http://iopscience.iop.org/0953-8984/12/38/303)

J. Phys.: Condens. Matter **12** (2000) 8257–8266. Printed in the UK PII: S0953-8984(00)14987-2

Embedded cluster calculations of metal complex impurity defects: properties of the iron cyanide in NaCl

Peter V Sushko†‡, Alexander L Shluger‡, Roger C Baetzold§ and C Richard A Catlow†

† The Royal Institution of Great Britain, 21 Albemarle Street, London W1X 4BS, UK
‡ Department of Physics and Astronomy, University College London, Gower Street, London WC1E 6BT, UK
§ Imaging Research and Advanced Development, Eastman Kodak Company, Rochester, NY 14650-2021, USA

Received 23 June 2000

Abstract. We present the results of calculations of the $\{[FeCl_{6-n}(CN)_n]^{m-} \times (V_{Na})_{5-m}\}^{5-}$ impurity complex incorporated in the NaCl crystal lattice. A number of characteristic defect configurations are calculated quantum mechanically using an embedded cluster method, and compared with the results of Mott–Littleton (ML) calculations. We investigate the electron affinity and the orientation of CN^- ligands. The dependence of vibrational frequencies of the CN stretching mode on the ligand orientation, charge of the impurity and the relative position of the ligands and the charge compensating vacancies are calculated. Analysis of these results demonstrates the ability of ML calculations to predict the relative stability of different configurations of this particular family of defects. Comparison of the ML and embedded cluster calculations reveals the contributions to the defect energy and stability.

1. Introduction

Impurity centres containing transition metal ions in different charge states play an important role in photographic materials [1, 2] and scintillators (see, for example, [3] and [4]). They substitute for the host lattice cation and are often surrounded by molecular ligands substituting for the nearest lattice anions. When an excess charge of the transition metal ion is compensated by cation vacancies, the impurity complexes in binary compounds may be described by a general formula $\{[ML_nA_{6-n}]^{m-} \times (V_{cat})_{5-m}\}^{5-}$, where M and L stand for the metal ion and its ligands, A is the lattice anion and V_{cat} is the cation vacancy, respectively. Typical examples of such impurity defects are $Cr(CN)_6^{3-}$ in NaBr [5] and $[OsCl_5(NO)]^{3-}$ in AgCl [6]. However, in many cases the number, configuration and even nature of the charge compensating species (e.g. vacancies or interstitial ions) are very difficult to establish (see, for example, discussion in [7–9]). Moreover depending on the preparation, the metal ion may be co-ordinated by a different number of molecular ligands, such as CN^- or NO^+, and these can have two average orientations. Therefore the total number of possible structural configurations of a metal complex impurity centre in some cases can reach several hundred. However, only a handful of them are statistically significant.

Optical, infrared and Raman spectroscopies as well as magnetic resonance based methods are often used to determine the structure and properties of these systems. However, the interpretation of experimental spectra is not always straightforward and benefits from

0953-8984/00/388257+10$30.00

knowledge of the defect structural configurations which are likely to be present in significant concentrations. These configurations can be determined theoretically, together with the general trends in optical absorption energies and vibrational frequencies as a function of the defect structural parameters. However, a huge number of possible configurations makes this an immense task for quantum-mechanical methods. Classical atomistic simulation techniques based on the Mott–Littleton (ML) method have long been used to study the structure and stability of impurity complexes in ionic crystals [10, 11]. A way forward could be to use this method to determine the relative energies of different defect configurations, and then to study the spectroscopic properties of the most stable structures. For that purpose it is important to establish whether one can trust classical calculations in the case of such complex defects. To address this question one needs to have a more accurate, quantum-mechanical method capable of predicting not only the relative stability of different defect structures, but also their spectroscopic properties.

To address some of these issues, in this paper we discuss the results of our calculations of the $\{[FeCl_{6-n}(CN)_n]^{m-} \times (V_{Na})_{5-m}\}^{5-}$ impurity complex incorporated in the NaCl crystal lattice. This defect has a range of features characteristic of complex defects mentioned above: molecular ligands, an open d shell of the 3d metal ion, many configurations of the charge compensating cation vacancies and different charge states, and has been extensively studied experimentally [12–15]. Our approach is to calculate a number of characteristic defect configurations quantum mechanically using a recently developed embedded cluster method [16], and to compare the predicted relative energies with the results of Mott–Littleton (ML) calculations of the same configurations. Then we investigate a number of defect properties, such as the electron affinity and orientation of CN^- ligands. We also study the dependence of vibrational frequencies of the CN^- stretching mode on this orientation, the charge of the impurity and the relative position of the ligand and the charge compensating vacancies, and compare them with the experimental data. Analysis of these results demonstrates the ability of ML calculations to predict the relative stability of different configurations of this particular family of defects, and gives a more general perspective on this approach. Comparison of ML and embedded cluster calculations reveals the most important contributions to the defect energy and stability. We discuss the criteria of applicability of this approach to similar defects.

2. Experimental and theoretical background

Dependent on the preparation conditions and temperature, a metal ion M substituting for the Na^+ ion in the NaCl lattice can be surrounded by a different number of CN^- ligands and cation vacancies. For example, the samples used in the recent study of the Yb^{2+}:$(CN^-)_n$ defect complexes in NaCl and other alkali halides [17] were grown from the melt and contain defects with the number of ligands n varying from zero to six. On the other hand, the samples containing Fe^{3+}:$(CN^-)_n$ complexes studied in [13] and [14] were grown at room temperature by slowly evaporating a saturated aqueous solution of the NaCl containing certain concentrations of $K_3Fe(CN)_6$. In the latter case, the complex $[Fe(CN)_6]^{3-}$, which is strongly bound in the aqueous solution, is supposed to be incorporated in the NaCl lattice intact. A similar method was used to prepare AgCl emulsions doped with $[Fe(CN)_6]^{4-}$ ions [18] and NaBr crystals doped with $[Cr(CN)_6]^{3-}$ ions [5]. Some other preparation techniques have been discussed in [12].

The EPR and vibrational spectra measured on the samples containing $[Fe(CN)_6]^{3-}$ and $[Cr(CN)_6]^{3-}$ impurity ions exhibited features which have been attributed to different configurations of charge compensating species [5, 18]. The $Fe(CN)_6^{3-}$ ion in NaCl occupies

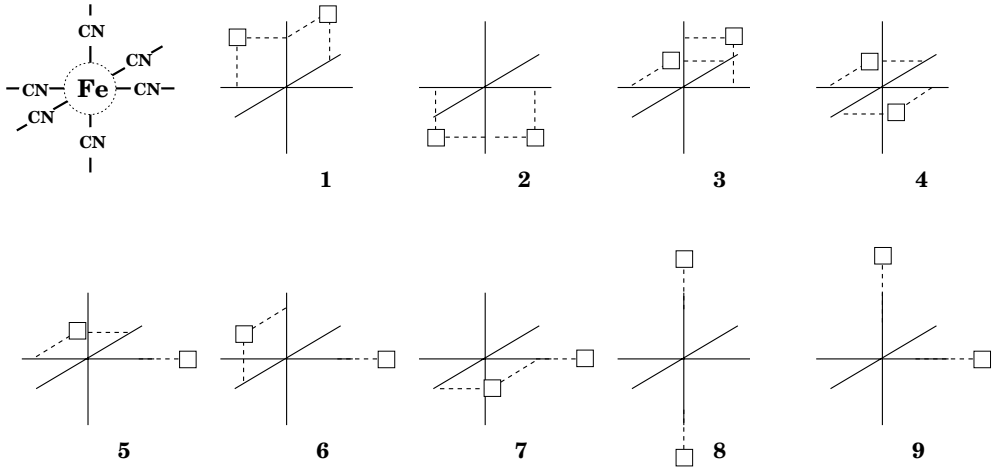

Figure 1. Schematic of nine possible configurations of the two cation vacancies at the (n) and (nn) sites with respect to the iron cyanide complex in NaCl.

seven lattice sites with six CN^- ions replacing six Cl^- ions, so that the octahedral $Fe(CN)_6^{3-}$ ion replaces the $NaCl_6^{5-}$ group in the host lattice. To keep the crystal electrically neutral, the defect is most likely associated with two cation vacancies. The electrostatic considerations suggest that most of the vacancies occupy the nearest (n) or next-nearest (nn) positions to the impurity ion centres. An alternative mechanism of charge compensation could be by Cl^- interstitial ions in the vicinity of the complex. However, as the formation energy of Schottky defects in NaCl is lower than that of Frenkel defects [19], the charge compensation by the interstitial anions is less probable. Nine possible configurations of the two cation vacancies at the (n) and (nn) sites are shown in figure 1.

The $Fe(CN)_6^{3-}$ ion is a typical covalent complex with a d^5 electronic configuration. It has a very large octahedral splitting (about 35 000 cm^{-1} [20]) due to the CN^- ligand field. Consequently, it is a low-spin t_{2g}^5 complex. The iron cyanides are diamagnetic in the case of an even number of electrons, as in the $Fe(CN)_6^{4-}$ ion, and have the magnetic susceptibilities of the order of magnitude corresponding to one free spin, i.e. $S = 1/2$ in the case of the $Fe(CN)_6^{3-}$ ion, as discussed by Van Vleck [21]. The three low-lying t_{2g} orbitals are split by the low-symmetry field due to different possible configurations of the charge compensating vacancies. The perturbation brought by the vacancies depends on their relative position with respect to the complex.

The paramagnetic $Fe(CN)_6^{3-}$ ion in NaCl and KCl has been studied by Wang *et al* [14, 15] using EPR and ENDOR at 4.2 K. Another extensive set of experiments was undertaken by Jain *et al* [13], who have studied the electronic and vibrational spectra of these ions in NaCl and KCl at liquid air temperature (113 K). These studies, however, arrived at contradictory conclusions regarding the local atomic structure of the defect centre in NaCl. According to [14] and [15], the most populated centre has the configuration 4 in figure 1, and the two other less populated configurations resolved by paramagnetic resonance were assigned to the configurations 3 and 6. In contrast, the analysis reported in [13] suggested that the most probable structure corresponds to the configuration 5. It should be noted that different temperature in these experiments is unlikely to cause such a disagreement in the results.

An important conclusion concerning the influence of cation vacancies on the energy of d orbitals has been made in [14]. To analyse this effect, the authors classified the positions

of the vacancies with respect to the d orbitals. The vacancy at the nearest cation site (the [110] site with respect to the iron ion) occupies either a position in the orbital plane along a lobe direction or a position that is 45 degrees off the orbital plane. If the former position is denoted as a subscript □ and the latter by a superscript □ then the energies of the d_{xy} and d_{xz} orbitals for configuration 4 may be denoted as $E_{\square\square}$ and $E^{\square\square}$, respectively. It has been observed that the relations $2(E^{\square}_{\square} - E_{\square\square}) = 2(E^{\square\square} - E^{\square}_{\square}) = E^{\square\square} - E_{\square\square}$ are nearly exactly obeyed in both NaCl and KCl. The deviation is less than 2.5% for NaCl and 0.5% for KCl. These relations demonstrate that the perturbations due to the vacancies are additive. A second interesting feature is that all three values $E^{\square\square} - E_{\square\square}$, $E^{\square\square} - E^{\square}_{\square}$ and $E^{\square}_{\square} - E_{\square\square}$ in KCl are between 92% and 94% of those in NaCl. These two percentage values are close to the ratio of the two lattice constants, which is 0.90. Such a good correlation indicates that the interaction between the Fe^{3+} and the vacancy is predominantly coulombic in nature.

On the theoretical front, the recent ML calculation [22] predicted configurations 4 and 3 to have the lowest and the second lowest total energies, while the third lowest defect centre structure corresponded to the configuration 2. Even more surprisingly, it appeared that the apparently unfavourable configuration 1 has a much lower energy than configurations 5 and 6 predicted in experimental studies [13] and [14] respectively. *Ab initio* quantum-mechanical calculations of Fe^{3+}:$(CN)_n$ centres in NaCl are absent. However, an extensive prototype calculations of these centres and also of the $[OsCl_5(NO)]^{2-}$ and $[RuCl_5(NO)]^{2-}$ centres in AgCl have been made in [22] and [6]. These studies recognized the importance of the lattice polarization in the determination of the structure, stability and electronic properties, in particular the electron affinity, of these centres. However, the electronic structure was calculated for the defect configurations determined by the ML method. This approach does not provide the complete geometry relaxation and does not account for the effect of the host lattice relaxation on the electronic structure of the QM cluster. These can be serious shortcomings since the structure and properties of complex defects described above are determined by the interplay of two main factors: (i) the interaction of compensating vacancies between themselves and with the impurity metal ion, including lattice polarization by these species, and (ii) the effect of vacancies on the electronic structure of the metal ion and ligands. The first contribution can be treated by the ML method, and, if the electronic structure of the metal–ligand complex does not depend appreciably on the position of vacancies, this method should be able to predict the relative energies of different configurations. One of the aims of this paper is to find out whether this is the case for iron cyanide complexes in NaCl. The method described below allows us to calculate the relative stability of different defect configurations taking into account their electronic structure.

3. Details of calculations

The embedded cluster method employed in this work has been described elsewhere [16]. Briefly, we consider a quantum cluster embedded in a large finite region of polarizable ions. Some of the ions closest to the quantum cluster are treated in the shell model [23] (region I) and they interact between themselves and the quantum cluster ions via the inter-atomic potentials [22]. In the shell model, an ion is represented by a point core and shell connected by a spring to simulate its dipole polarizability. The positions of the cores and shells of each of these ions are optimized in response to the changes in the charge density distribution within the quantum cluster to minimize the total energy of the whole system. The rest of the point ions outside region I form region II of fixed non-polarizable ions, which provide the correct electrostatic potential distribution in the quantum cluster and in region I. This approach has the flexibility necessary to model complex structures and the advantage of being easily portable with many

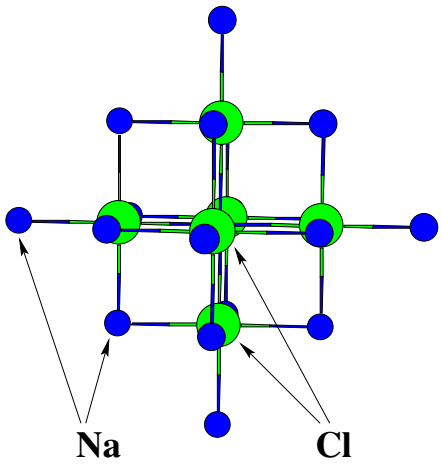

Figure 2. The QM cluster used in the embedded cluster calculations. The $Na_{19}Cl_6$ cluster shown in the figure represents the host crystal. In defect calculations, the central Na ion was replaced by Fe and one or several Cl ions were replaced by CN ligands (see figure 1).

of the standard quantum-mechanical programs. The crystalline potential on individual ions in this approach is determined up to a constant, which depends on the shape and size of the region. This, however, does not affect the relative energies we are interested in this work.

The electronic structure calculations are performed using the Gaussian98 code [24], which is interfaced with a special code developed in our group for calculation of forces on the shell-model ions. Since the lattice outside the QM cluster is represented by point charges (including cores and shells), the polarization potential is included in the electronic structure calculations via the matrix elements of these charges. The scheme of the total energy calculation is described in [16]. The total forces acting on each centre, i.e. the QM ions and the classical cores and shells, are calculated by differentiating the total energy with respect to the coordinates of corresponding species. This allows us to minimize the system total energy simultaneously with respect to the electronic coordinates and the positions of QM ions and classical ions and to avoid the time-consuming 'self-consistency' procedure [25]. The energy minimization is performed using the BFGS optimization procedure [26] via the known direction of relaxation at the previous minimization step and total forces. The calculation is completed when the changes in the system total energy, coordinates of all species, and forces on each species become smaller than 10^{-5} eV, 0.0003 Å, and 0.03 eV $Å^{-1}$, respectively.

The cubic nano-cluster, used to model bulk NaCl, has $25 \times 25 \times 25$ ionic centres. Formal ionic charges have been used for all fully coordinated ions; charges on ions at the surface, edge and corner sites of the nano-cluster are $1/2$, $1/4$ and $1/8$ of their formal values. We checked that this set-up reproduces the electrostatic potential and the electric field on all ions in region I with the accuracy of 10^{-6} eV and 10^{-5} eV $Å^{-1}$, respectively. A spherical region I of the radius 16.7 Å, containing more than 900 atoms, was situated at the centre of the nano-cluster. Most of the calculations were made using the QM cluster which is equivalent to the $Na_{19}Cl_6$ cluster of the host crystal (see figure 2). One or several anions of this cluster have then been replaced by CN ligands.

Throughout the calculation we have used the density functional (DF) method and the B3LYP density functional [27]. In all cases, a full electron basis set was used for the central cation and its six ligands, while other cations have been described using an effective core

Table 1. Basis sets used in the present study.

Basis	Fe	C, N	Cl
A	6-31G	6-31G	6-31G
B	6-311G	6-311G	6-311G
C	6-311G	6-311G*	6-311G
D	6-311G	6-311G*	6-311G*

pseudo-potential [28] and one s-type basis function. To check the dependence of the results on the quality of the basis set, in several cases we have employed several full electron basis sets listed in table 1.

4. Results of calculations

4.1. Relative energies of defect configurations of ferrocyanide complex

Fe^{3+} ions in NaCl can trap electrons creating stable closed shell complexes, such as $Fe(CN)_6^{4-}$, which require only one cation vacancy for charge compensation. Study of these simpler centres allows us to obtain some initial insight into the interplay between the metal, ligand and vacancy interactions in the crystalline matrix. The results of the calculations of the $[FeCl_6]^{4-}$, $[FeCl_5(CN)]^{4-}$ and $[Fe(CN)_6]^{4-}$ ions compensated by one cation vacancy are summarized in table 2. It presents the relative energies of different configurations of the complex with vacancies at the nearest (n) and next-nearest (nn) neighbour sites. These results allow us to make the following conclusions. (i) If there is no CN^- ligand present, the field due to surrounding Cl^- ions is not strong enough to cause large t_{2g}–e_g splitting of the Fe^{2+} ion states and, consequently, the metal ion has $t_{2g}^4 e_g^2$ electronic configuration and high spin $S = 2$. It is difficult to say conclusively whether the cation vacancy occupies (n) or (nn) site, because the difference in total energies for these two configurations is very small. Even though the electrostatic interaction of the negative vacancy with the positive ion is larger if the vacancy is at the (n) site, this is compensated by a larger repulsive interaction of the vacancy at the (n) site with electrons of the t_{2g} orbitals and a larger lattice polarization energy for the vacancy at the (nn) site. (ii) If the CN^- ligand is present, its size plays an important role in the local structure of the complex. In the case when the ligand is between the Fe^{2+} ion and the vacancy, a negatively charged N atom is closer to the vacancy site than the Cl^- ion in the case of $[FeCl_6]^{4-}$, consequently the repulsive vacancy–ligand interaction is much stronger. In addition, the Fe–CN distance is smaller than the Fe–Cl distance in $[FeCl_6]^{4-}$, which leads to an additional energy increase according to Pauli repulsion. The CN ligand interacts strongly with the electrons of the Fe^{2+} ion, significantly reducing the splitting between the high-spin and the low-spin electronic configurations. (iii) For the case where all six Cl ions are replaced by CN ligands, the relative energy for the vacancy to occupy an (n) site becomes only slightly larger than in the case of one ligand. (iv) Flipping of the CN ligand so that its 'N end' is oriented towards the central Fe ion has no effect on the (n) versus (nn) relative stability. (v) The Fe–CN orientation of the ligands is by about 0.6 eV per one ligand molecule more favourable than Fe–NC orientation independent of the position of the vacancy. (vi) Finally, the relative energies are almost independent of the basis set although the total energies change significantly.

4.2. Structure of the ferricyanide complex

The relative energies of the nine non-equivalent configurations of the $[Fe(CN)_6]^{3-}$ ion compensated by two cation vacancies are presented in table 3. The first column in table 3

Table 2. Relative energies (eV) of local structures with the cation vacancy at the [200] site with respect to that at the [110] site for several metal complexes. (The positive sign corresponds to the configuration with the cation vacancy at the [110] site being more stable than that at the [200].) Note that the energies are given with respect to the Fe–CN and Fe–NC orientations of the ligands, respectively (see also text for discussion).

		$[FeCl_5(CN)]^{4-}$[a]		$[Fe(CN)_6]^{4-}$	
Basis	$[FeCl_6]^{4-}$	Fe–CN	Fe–NC	Fe–CN	Fe–NC
A	−0.02	0.37	0.37	0.55	0.56
B	0.03	0.33	0.29	0.52	0.47
C		0.26	0.24		
D		0.27	0.25		

[a] In this configuration the CN^- ligand occupied the [100] lattice site, which corresponds to the smallest possible distance between the ligand and the vacancy. It is expected that for configurations with larger ligand–vacancy distances, the vacancy is more likely to occupy the (nn) site rather than the (n) site.

Table 3. The relative energies (eV) of the nine non-equivalent configurations of the $\{[Fe(CN)_6]^{3-} \times 2(Vac_{Na^+})\}^{5-}$ defect centre (see figure 1) with respect to the most stable configuration 4.

	This work					Experiment	
Config.	Basis A	Basis B	Estimate[a]	Estimate[b]	ML [22]	[13]	[14]
1	0.323	0.326	0.242	1.833	0.339		
2	0.185	0.180	0.247	0.759	0.298		
3	0.051	0.052	0.033	0.284	0.061		II
4	0.000	0.000	0.000	0.000	0.000		I
5	0.644	0.621	0.737	3.028	0.370	*	
6	0.728	0.710	0.805	3.505	0.438		III
7	0.973		1.023	5.024	0.640		
8	1.284		1.526	5.905	0.750		
9	1.362		1.601	6.442	0.790		

[a] The energies have been deduced from binding energies of the $[Fe(CN)_6]^{3-}$ ion with a single vacancy (see text for more details).
[b] The energies have been calculated for the Coulomb interaction of the two vacancies with the Fe^{3+} ion and with each other (see text for more details).

refers to the number of configurations shown in figure 1. The relative energies in the second and third columns were calculated using the embedded cluster approach. These energies can be compared to the results of previous Mott–Littleton calculations [22] summarized in column six. The meaning of the values presented in the fourth and fifth columns is explained later. Finally, the two last columns present the results of the experimental studies discussed in section 2.

Comparison of the different theoretical and experimental results allows us to make the following observations: (i) all theoretical calculations produce the same ordering of the stability and similar values of the relative energies; (ii) the relative energies calculated using basis sets A and B are almost identical. In other words, the details of the defect electronic structure missed in the Mott–Littleton calculation are not essential for identifying the most stable configuration.

4.3. Effect of the atomic structure on the C–N stretching mode

The experimental studies show that the C–N stretching mode is very sensitive to the atomic and electronic structures of its local environment. Apart from the already mentioned study

Table 4. Frequencies of C–N stretching vibrations of iron cyanides.

Defect ion	Configuration	C–N stretching (cm^{-1})
$[Fe(CN)_6]^{4-}$	$(CN)_5$–Fe–CN	2117.3
$[Fe(CN)_6]^{4-}$	$(CN)_5$–Fe–NC	2153.1
$[Fe(CN)_6]^{3-}$	Config. 4 in fig. 1	2178.8

Table 5. Electron affinities of several $[Fe(CN)_6]^{3-}$ complexes (eV).

Defect ion	Configuration	Electron affinity
$[Fe(CN)_6]^{3-}$	4	4.668
$[Fe(CN)_6]^{3-}$	3	4.665
$[Fe(CN)_6]^{3-}$	6	4.746

of vibrational spectra of NaCl and KCl crystals doped with iron hexacyanides by Jain *et al* [13], an extensive study of the C–N stretching fundamentals for $[Fe(CN)_6]^{3-}$ and $[Fe(CN)_6]^{4-}$ complexes in several alkali halide hosts has been made by Duncan and Percival [12]. They have demonstrated that the C–N stretching in alkali halides has a multiplet structure, and that the C–N stretching frequencies for the $[Fe(CN)_6]^{3-}$ ion in NaCl are about 70 cm^{-1} larger that those for the $[Fe(CN)_6]^{4-}$ ion. To calculate the latter relatively small shift could be a further test of our model. We have also checked whether flipping of the CN^- ion affects its vibrational frequency.

The C–N stretching frequencies were calculated for three systems shown in table 4 for one of the CN^- ions of the complex. The fundamental frequency is close to the experimental value of about 2130 cm^{-1} [13]. The CN stretching for the $[Fe(CN)_6]^{3-}$ ion has higher frequency than for the $[Fe(CN)_6]^{4-}$ ion and the magnitude of the frequency shift is close to the experimentally observed value of 70 cm^{-1} [12]. This is due to the stronger electrostatic interaction of the positive central ion with its negatively charged ligands. However, this agreement is qualitative because the complete multiplet structure of the CN stretching mode was not calculated. It also follows from the data presented in table 4 that the flipping of the CN molecular ion should be associated with appreciable frequency shift, which may well be observed using existing experimental methods. This shift is expected to be larger for the $[Fe(CN)_6]^{3-}$ ion.

4.4. Dependence of electron affinities on configuration

The results of our calculations suggest that the ferricyanide ion in NaCl has a large electron affinity (EA) of about 4.7 eV. Such a large value of the EA may be explained by empty states, which appear in the region corresponding to the crystal band gap in our calculations. A trapped electron is mostly associated with the Fe^{3+} ion, converting it to Fe^{2+}. Taking into account the conclusion made in [14] about the additive effect of the vacancies on the complex properties, one would expect that the electron affinity depends on the distance from the iron ion to the vacancy. This dependence was indeed observed in our calculations. The calculated electron affinities for configurations 4, 3 and 6 corresponding to centres I, II and III identified in [14] are presented in table 5. Configurations 4 and 3 have both vacancies at (n) sites and, consequently, electron affinities for these configurations are almost identical. In configuration 6 one vacancy occupies an (n) site and the other an (nn) site. This change in the average distance between the vacancies and the iron ion leads to a slightly larger electron affinity.

5. Discussion

Our calculations support the conclusion made in [14] that the most stable atomic structure of $[Fe(CN)_6]^{3-}$ corresponds to configuration 4 and the second most stable to configuration 3 in figure 1. The same conclusion has been reached in [22]. It is somewhat unexpected that configuration 1, which was ruled out in both experimental studies, is more stable than configurations 5 and 6. In order to understand this, we estimated the energies of nine configurations taking into account only the electrostatic interaction of the vacancies and the Fe^{3+} ion. The vacancies were represented by negative point charges equal to -1 e, and the Fe^{3+} ion by a positive point charge +3 e (e is the electron charge). All charges were fixed at the corresponding ideal lattice sites. The calculated energies (shifted to obtain the relative values) are presented in the fifth column in table 3. It can be seen that the relative energy of configuration 1 is smaller than those of configurations 5 or 6 and, therefore, it should have been considered in the interpretation of the experimental results. We should note that in the ligand–field analysis undertaken in [14] to interpret the results of the EPR experiment only configuration t_{2g}^5 for the Fe^{3+} was considered, while in our calculations an appreciable admixture of the e_g states appears for the low-symmetry configurations. This factor could have misled the interpretation of the EPR experiments.

The choice between centres of the D_{2h} and C_s symmetries, i.e. between configurations 4 and 5, respectively, has been made in [13] on the basis of the relatively small magnitude of the splitting of the CN stretching mode ν_6, and the presence of additional Raman active modes, ν_1 and ν_3. The latter modes are inactive in the case of the D_{2h} symmetry, but become active in the case of lower symmetry. In fact, both of these observations could be interpreted in a different way. Indeed, if the cation vacancy is at the (nn) site, i.e. along the Fe–CN axis, its negative charge 'pushes' the CN^- ligand towards the Fe^{3+} ion, which is likely to affect the vibrational energy of the stretching mode more than if the vacancy were at the (n) site. Therefore, the relatively small magnitude of the stretching mode splitting should support the view that D_{2h} symmetry of the complex is more favourable. The presence of the modes ν_1 and ν_3, which are much less intense than the CN stretching mode, could be due to other configurations present in small concentrations. For example, these modes become Raman active if the symmetry of the complex is C_2, which corresponds to configuration 3. We have to note that, apart from ENDOR, which has been used to study configuration 4, the experimental techniques employed in [13] and [14] do not provide direct structural information and have to be supported by other studies.

Early semi-empirical calculations of the electronic structure of hexacyanides [29] suggested that the molecular orbitals associated with ligands and those associated with the central metal ion can hybridize leading to charge transfer between the metal ion and the ligands. However, redistribution of the charge density due to different configurations of vacancies proved to be insignificant in our calculations and, therefore, ligands can be treated as closed shell systems. This and other results presented above prompted us to explore another approach to minimize efforts of identification of the most stable configuration of the $[Fe(CN)_6]^{3-}$ ion. For this purpose we have calculated binding energies of a single vacancy with the $[Fe(CN)_6]^{3-}$ ion for two non-equivalent configurations of vacancies at (n) and (nn) sites using the embedded cluster approach. The repulsion of two vacancies in NaCl for the nine configurations shown in figure 1 was calculated using the Mott–Littleton approach and the GULP code [30]. The binding energy of the $[Fe(CN)_6]^{3-}$ ion with two vacancies was then estimated as the sum of the binding energy with the single vacancy and the repulsion energy of the two cation vacancies. The binding energies were shifted to obtain the relative energies, which are summarized in the fourth column of table 3. Good agreement between the estimated energies and those calculated

for the whole system suggests that this procedure can be applied for preliminary identification of the most stable configurations of the system. This result also supports the conclusion made in [14] that the perturbation due to the cation vacancies has an additive character.

To summarize, our results suggest that the order of the relative energies of different configurations of the $[Fe(CN)_6]^{3-}$ ion associated with two cation vacancies is largely determined by the electrostatic interaction of ions composing the system and the lattice polarization. The Mott–Littleton approach to calculation of the structure of similar complexes is valid if the electronic structure of the complex does not undergo qualitative changes with the change of the environment. Combination of quantum-mechanical embedded cluster and classical ML calculations can provide an effective and reliable way to study the structure and properties of such complexes.

Acknowledgments

PVS is grateful to Eastman Kodak for financial support. We would like to thank L N Kantorovich, I V Abarenkov and I I Tupitsyn for useful comments and help in calculations. We are grateful to R S Eachus for stimulating discussions and valuable comments on the manuscript.

References

[1] Forster L S 1991 *Adv. Photochem.* **16** 215
[2] Marchetti A P and Eachus R S 1992 *Adv. Photochem.* **17** 145
[3] Wegh R T, Donker H, Meijerink A, Lamminmäki R J and Hölsä J 1997 *Phys. Rev.* B **56** 13 841
[4] Wegh R T, Donker H, Oskam K D and Meijerink A 1999 *Science* **283** 663
[5] Hermanowicz K 1997 *J. Phys.: Condens. Matter* **9** 1369
[6] Eachus R S, Baetzold R C, Pawlik T D, Poluektov O G and Schmidt J 1999 *Phys. Rev.* B **59** 8560
[7] Wang D M and de Boer E 1989 *Phys. Rev.* B **39** 11 272
[8] Visser R, Andriessen J, Dorenbos P and van Eijk C W E 1993 *J. Phys.: Condens. Matter* **5** 5887
[9] Vercammen H, Schoemaker D, Briat B, Ramaz F and Callens F 1999 *Phys. Rev.* B **59** 11 286
[10] Corish J, Catlow C R A, Jacobs P W M and Ong S H 1982 *Phys. Rev.* B **25** 6425
[11] Foot J D, Colbourn E A and Catlow C R A 1988 *J. Phys. Chem. Solids* **49** 1225
[12] Duncan J F and Percival H J 1968 *Aust. J. Chem.* **21** 2175
[13] Jain S C, Warrier A V R and Sehgal H K 1973 *J. Phys. C: Solid State Phys.* **6** 193
[14] Wang D M, Meijers S M and Boer E D 1990 *Mol. Phys.* **70** 1135
[15] Wang D M and Boer E D 1990 *J. Chem. Phys.* **92** 4698
[16] Sushko P V, Shluger A L and Catlow C R A 2000 *Surf. Sci.* **450** 153
[17] An C P, Dierolf V and Luty F 2000 *Phys. Rev.* B **61** 6565
[18] Olm M T, Eachus R S and McDugle W G 1993 *Bulgar. Chem. Commun.* **26** 1993
[19] Lushchik C B and Lushchik A C 1989 *Decay of Electronic Excitations with Defect Formation in Solids* (Moscow: Nauka)
[20] Jorgensen C K 1962 *Absorption Spectra and Chemical Bonding in Complexes* (Oxford: Pergamon)
[21] Van Vleck J H 1935 *J. Chem. Phys.* **3** 807
[22] Baetzold R C 1997 *J. Phys. Chem.* B **101** 1130
[23] Dick B G and Overhauser A W 1958 *Phys. Rev.* **112** 90
[24] Frisch M J *et al* 1998 *Gaussian 98 edition E1* (Pittsburgh, PA: Gaussian Inc.)
[25] Shluger A L, Harker A H, Puchin V E, Itoh N and Catlow C R A 1993 *Modelling Simulation Mater. Sci. Eng.* **1** 673
[26] Dennis J E and Schnabel R B 1983 *Numerical Methods for Unconstrained Optimization and Nonlinear Equations* (Englewood Cliffs, NJ: Prentice-Hall)
[27] Becke A D 1993 *J. Chem. Phys.* **98** 5648
[28] Wadt W R and Hay P J 1985 *J. Chem. Phys.* **82** 284
[29] Alexander J J and Gray H B 1968 *J. Am. Chem. Soc.* **90** 4260
[30] Gale J D 1997 *J. Chem. Soc. Faraday Trans.* **93** 69